N-Substituted Benzene-1-Urea-3,5-Biscarboxamide (BUBA): Easily Accessible C 2 -Symmetric Monomers for the Construction of Reversible and Chirally Amplified Helical Assemblies

Yan Li, Ludovic Dubreucq, Bruno G Alvarenga, Matthieu Raynal, Laurent Bouteiller

N-substituted benzene-1-urea-3,5-biscarboxamide (BUBA): easily accessible C_2-symmetric monomers for the construction of reversible and chirally-amplified helical assemblies

Yan Li,[a] Ludovic Dubreucq,[a] Bruno G. Alvarenga,[a,b] Matthieu Raynal*[a] and Laurent Bouteiller[a]

Abstract: Non C_3-symmetric supramolecular helices are gaining interest for the design of hierarchical assemblies, for the compartmentalization or the self-assembly of polymer chains and for application in asymmetric catalysis. We introduce *N*-substituted benzene-1-urea-3,5-biscarboxamide (BUBA) monomers, which consist of one urea and two carbon-connected amide functions linked to an aromatic ring, as an easily-accessible class of C_2-symmetric supramolecular synthons. In apolar solvents, BUBA monomers assemble into long helical assemblies by means of hydrogen-bonding and aromatic interactions, as assessed by several analytical techniques. In order to probe the influence of the urea function, BUBA and related benzene-1,3,5-tricarboxamide (BTA) helical polymers have been compared in terms of their thermodynamics of formation, stability, reversibility and chirality amplification properties. Like BTA, BUBA monomers form long helices reversibly through a highly cooperative mechanism and the helicity of their assemblies is governed by chiral amplification effects. However, precise quantification of their properties reveals that BUBA monomers assemble in a more cooperative manner. Also, chirality amplification operates to a higher extent in BUBA helices as probed by both sergeants-and-soldiers and majority-rules experiments. Compatibility between urea and amide functions also allows the formation of co-assemblies incorporating both BUBA and BTA monomers. Importantly, a small amount of chiral BUBA monomers in these co-assemblies is enough to get single-handed helices which paves the way towards the development of functional supramolecular helices.

Introduction

Inspired by non-covalent helical biomacromolecules such as DNA, collagen and F-actin, huge efforts have been devoted to the synthesis of artificial helices,[1] not only in order to better control their mechanism of formation but also as a result of their exciting properties as asymmetric catalysts,[1-2] as sensors,[3] as templating agents,[4] as lyotropic,[5] or ferroelectric materials,[6] as organic luminophores,[7] and as spin filters.[8] The predictable assembly of small building blocks by means of directional non-covalent interactions constitutes the method of choice for the construction of supramolecular helical assemblies. Notably, aromatic scaffolds connected with hydrogen-bonding groups[9] are known that stack upon each other through a cooperative mechanism and yield long one-dimensional supramolecular polymers in solution.[10] Moreover, chirality induction and amplification phenomena are operative in these dynamic systems and are key elements for the preparation of functional assemblies.[11]

Benzene-1,3,5-tricarboxamide monomers (BTA, Chart. 1) are ubiquitous supramolecular synthons for the construction of helical stacks.[12] Adjacent monomers are connected by means of three hydrogen-bonds and an aromatic interaction between the BTA rings. The main advantages of the BTA platform are the simplicity of the BTA chemical structure, the predictability and cooperativity of the assembly process and the strong chirality amplification properties governing the formation of the helical assemblies. *N*,*N*',*N*''-substituted C_3-symmetric BTA monomers are easily prepared by direct functionalization of benzene-1,3,5-tricarboxylic acid or its acyl chloride derivative and have found numerous applications in various fields of chemical sciences. When it comes to imparting BTA assemblies with specific properties, the integration of one or two functional groups on the BTA unit is highly desired. C_2-symmetric BTA monomers have notably been used in organic solvents as assembling ligands for performing asymmetric reactions,[13] as building blocks for the design of hierarchical structures,[14] and as pendant units to trigger the folding or the self-assembly of polymer chains.[15] These desymmetrized BTAs are obtained *via* the incomplete hydrolysis of trimethyl benzene-1,3,5-tricarboxylate,[16] the partial esterification of trimesic acid,[15e] or the stoichiometrically-biased addition of alkyl amines to trimesic chloride,[13a, 17] all these routes being lengthy and modestly efficient.[18] Avoiding such desymmetrization protocols will significantly leverage the synthetic effort towards C_2-symmetric assembling units and their corresponding helical assemblies.

C_2-symmetric starting materials such as 3,5-dinitroaniline,[19] 3,5-dinitrobenzoic acid,[20] and 5-aminoisophthalic acid[19b, 21] not only facilitate the preparation of disk-like molecules with two different side chains but also allow to connect urea and amide functions to the same aromatic ring. However, the influence of different recognition units on the assembly properties of these monomers has been scarcely investigated. Meijer and co-workers reported on unsymmetrical “gallic” disks composed of two urea and one nitrogen-connected amide functions and found that the urea groups promoted the formation of columnar helical aggregates in dilute alkane solutions.[19a] However, the supramolecular helices formed by these monomers or by related C_3-symmetric benzene-1,3,5-trisureas[22] are poorly dynamic and display modest chirality amplification properties. Clearly, a balance has to be found between the stronger hydrogen bond-forming capability of urea functions and the dynamics of the assemblies in order to maintain (or outperform) the properties observed in BTA helices. Here, we introduce *N*-substituted benzene-1-urea-

[a] Sorbonne Université, CNRS, Institut Parisien de Chimie Moléculaire, Equipe Chimie des Polymères, 4 Place Jussieu, 75005 Paris (France) matthieu.raynal@upmc.fr.
[b] Department of Physical-Chemistry, Institute of Chemistry, University of Campinas − UNICAMP, Campinas (Brazil)

Supporting information for this article is given via a link at the end of the document.

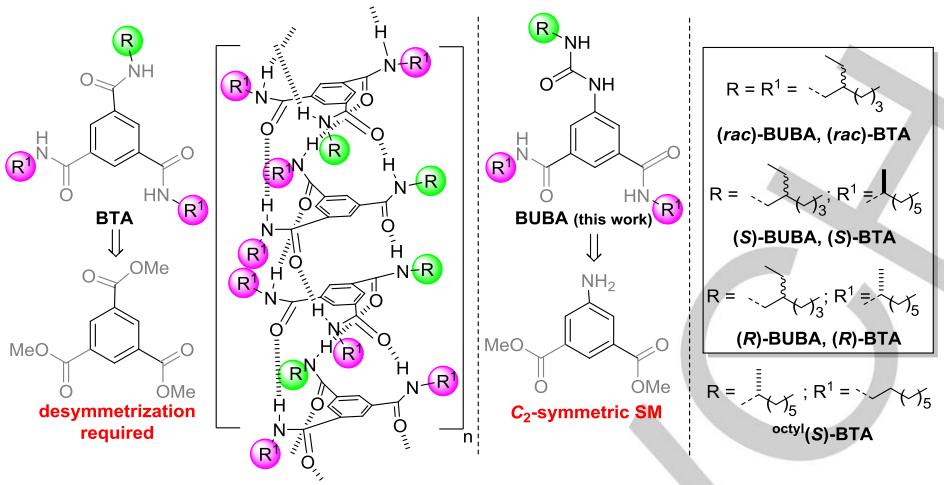

Chart 1 Molecular structures of the monomers investigated throughout this paper. Representation of the supramolecular BTA helices (the R and R^1 groups are assumed to be randomly distributed at the periphery of the helices). **(*rac*)-BUBA** is racemic by synthesis and thus consists of the stereoisomers (S_{urea},*S*,*S*), (S_{urea},*R*,*S*), (S_{urea},*R*,*R*), (R_{urea},*S*,*S*), (R_{urea},*R*,*S*), (R_{urea},*R*,*R*) in a 1:2:1:1:2:1 ratio. **(*rac*)-BTA** is racemic by synthesis and thus consists of the stereoisomers (*S*,*S*,*S*), (*S*, *S*, *R*), (*R*,*R*,*S*), (*R*,*R*,*R*) in a 1:3:3:1 ratio. **(*S*)-BUBA** and **(*S*)-BTA** consist of a 1:1 mixture of the (*S*,*S*,*S*) and (*R*,*S*,*S*) stereoisomers. The assembly properties of **(*S*)-BTA** will be compared to that of its structural analogue ^{octyl}**(*S*)-BTA**, reported in the literature.[23]

3,5-biscarboxamide (BUBA, Chart 1) monomers, comprising one urea function and two carbon-connected amide groups, as a new family of easily-accessible C_2-symmetric supramolecular synthons. The assembly behaviour of BUBA monomers has been probed by several analytical techniques and compared to that of BTA analogues in order to precisely assess the influence of the urea function on the structure and properties of the supramolecular helices. Our study reveals that BUBA monomers form long, stable and reversible helical assemblies in apolar solvents. The presence of the urea function positively influences the extent of cooperativity and the degree of chirality amplification operating in these helical supramolecular systems. The compatibility between the urea and amide functions is further exploited to generate single-handed BUBA/BTA co-assemblies which will foster the development of functional supramolecular helices.

Results and Discussion

Synthesis of the monomers

Gram-scale synthesis of BUBA monomers has been achieved in three steps from dimethyl 5-aminoisophthalate, a cheap starting material (SM), through conventional synthetic protocols with overall yields ≥ 50% (see Fig. 1 for **(*S*)-BUBA**). Branched alkyl side chains ((*rac*)-2-ethylhexyl for **(*rac*)-BUBA** and both (*rac*)-2-ethylhexyl and optically pure 1-methylheptyl for **(*S*)-BUBA** and **(*R*)-BUBA**) have been preferred over linear ones to favour the formation of one-dimensional soluble assemblies.[24] After recrystallization in acetonitrile, **(*rac*)-BUBA** is obtained as an amorphous solid and **(*S*)-BUBA** and **(*R*)-BUBA** are crystalline solids. The high purity of the BUBA monomers is confirmed by ^{1}H NMR, ^{13}C NMR and High-Resolution Mass Spectrometry analyses. As a result of the chiral racemic nature of the 2-ethylhexyl side chain, **(*rac*)-BUBA** is a racemic mixture of 6 stereoisomers and **(*S*)-BUBA** consists of a 1:1 mixture of the (*S*,*S*,*S*) and (*R*,*S*,*S*) stereoisomers (see caption of Chart 1).

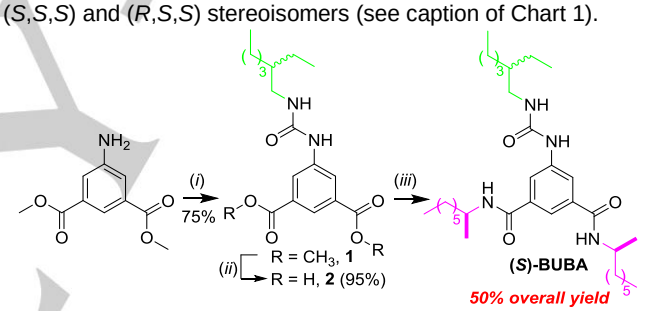

Figure 1 Synthesis of **(*S*)-BUBA**. (*i*) Triphosgene/DIEA/2-ethylhexylamine, (*ii*) LiOH/H_2O and (*iii*) EDC·HCl/DMAP/(*S*)-2-octylamine.

BTA analogues of these BUBA monomers have been prepared with the purpose of precisely probing the influence of the urea function on the structure of the assemblies as well as on their chiroptical and dynamic properties. C_3-symmetric **(*rac*)-BTA** is obtained in a single step according to literature.[25] For C_2-symmetric BTAs, a well-established route has been followed which consists in the partial hydrolysis of trimethyl benzene-1,3,5-tricarboxylate[16] and subsequent amidation − hydrolysis − amidation steps. This four-steps procedure furnishes **(*S*)-BTA** and **(*R*)-BTA** with an overall yield of 10% and 6%, respectively, as a result of the limited efficiency of the desymmetrization step (see Chart S1 for the compared syntheses of **(*S*)-BUBA** and **(*S*)-BTA**). Starting from a C_2-symmetric starting material thus allows BUBA monomers to be obtained in significantly higher yields than their BTA analogues.

Structure of the self-assemblies

The structure of **(*rac*)-BUBA** self-assemblies has been probed by means of Small-Angle Neutron Scattering (SANS), Fourier-Transform Infrared (FT-IR), Circular Dichroism (CD) and UV-Vis

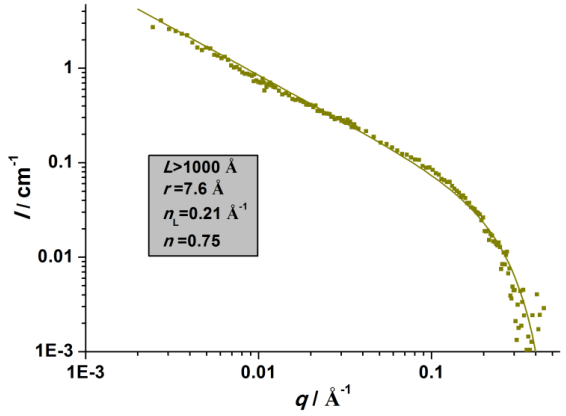

Figure 2 SANS analysis (■) of ***(rac)*-BUBA** (6.0 g.L^{-1}, 10.8 mM) in C_7D_8 at 293 K. The curve was fitted (⟶) according to the form factor for rigid rods of infinite length with a circular cross section and a uniform scattering length density (*L* =length, *r* =radius, n_L =number of molecule per unit length, *n*= number of molecule in the cross-section assuming a repeat distance of 3.6Å).[26]

absorption analyses. The q^{-1} dependence of the scattering intensity at low q values is indicative of the presence of rigid one-dimensional objects (Fig. 2). Fitting of the SANS data shows that these objects are very long (length>1000 Å, DP_w>275) and contain a single molecule of BUBA in the cross-section (r = 7.6 Å,[27] n=0.75).[26] FT-IR analysis of a 5 mM solution of ***(rac)*-BUBA** in decahydronaphthalene (DHN, Fig. 3b) provides information about the nature of the hydrogen-bond network in BUBA assemblies. Two distinct absorption maxima are detected in the N-H region, at ν=3369 cm^{-1} and ν=3250 cm^{-1}, which correspond to bonded urea N-H and bonded amide N-H functions, respectively, by analogy with the FT-IR spectra of **4TEHU** (Chart S2) and ***(rac)*-BTA** (Fig. 3a). In fact, models for free urea and amide moieties have also been recorded (Fig. S1) which allows for a quantitative analysis of the proportion of free N-H groups in BUBA self-assemblies. The resulting simulated FT-IR spectrum is shown in Fig. 3b (see Fig. S2 for its deconvolution into bands for bonded and free groups). The following points concerning the structure of BUBA self-assemblies are inferred from these analyses: (i) most of the urea (99%) and amide (97%) functions are bonded, (ii) the free urea and amide groups are not located at the chain ends[28] but can be rather considered as "defects" in the hydrogen-bond network since their amount does not decrease when the concentration in BUBA monomers increases (Fig. S1) and, (iii) the bonded urea N-H band in the experimental spectrum is blue-shifted comparatively to that in the simulated spectrum which indicates that the N-H urea groups in BUBA polymers are less strongly associated than in **4TEHU** assemblies.

(*S*)-BUBA and **(*R*)-BUBA** form helical assemblies in DHN as probed by CD analyses (Fig. 4). Four CD signals are observed with maxima at 299 nm (|Δε|=3 L.mol^{-1}.cm^{-1}), 250 nm (|Δε|=16 L.mol^{-1}.cm^{-1}), 224 nm (|Δε|=28 L.mol^{-1}.cm^{-1}) and 207 nm (|Δε|=66 L.mol^{-1}.cm^{-1}) whereas no detectable signals are seen in the molecularly-dissolved state. Interestingly, the Cotton effect at 299 nm is related to an electronic transition (π−π* or n−π*) of the urea carbonyl group.[29] The marked difference between the CD spectra of **(*S*)-BTA** (Fig. S4) and **(*S*)-BUBA**, the presence of an

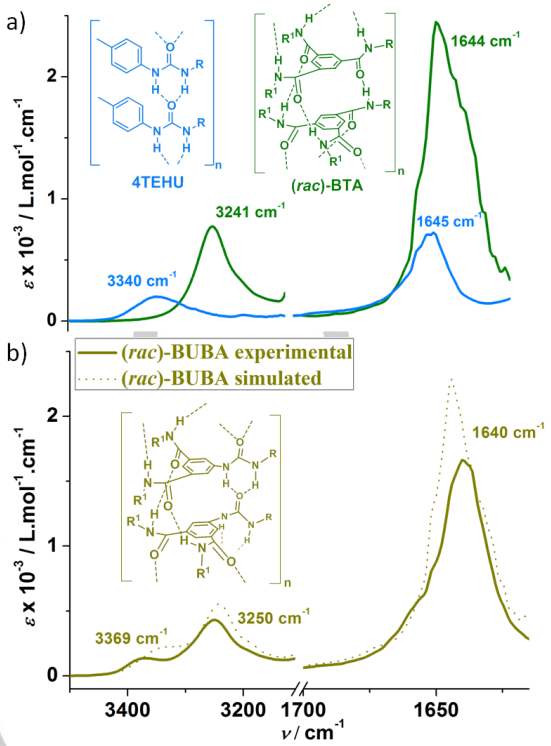

Figure 3 (a) FT-IR analyses of ***(rac)*-BTA** (10 mM, toluene) and 1-(4-tolyl)-3-(2-ethylhexyl)-urea (**4TEHU**, 25 mM, DHN), symmetric "models" for fully bonded amide and urea functions, respectively. (b) FT-IR analysis of ***(rac)*-BUBA** (5 mM, DHN, 293 K) and simulated spectrum aimed at probing the hydrogen bond network of BUBA assemblies as discussed in the main text and in the SI (Figs. S1 and S2).

ECD band exclusively attributed to the urea function and the FT-IR analyses (*vide supra*) all corroborate the involvement of the urea group in the hydrogen-bonding network of BUBA assemblies. The main UV-Vis absorption band is hypsochromically shifted upon assembly (dotted arrow in Fig. 4 bottom, Δλ=9 nm) which indicates a H-type aggregation mode for BUBA monomers. The CD spectra of **(*S*)-BUBA** and **(*R*)-BUBA** are, as anticipated, mirror images but it remains to be determined whether their handedness is identical to **(*S*)-BTA** and **(*R*)-BTA** respectively since it has been previously found that subtle modification in the structure of the monomer can lead to inversion in the sense of rotation of the respective assemblies.[23a, 23c-e]

The above-mentioned analyzes provide a precise picture of the structure adopted by BUBA self-assemblies: they are one-dimensional with a single molecule in the cross-section and they form helices with a preferred handedness in which most of amide and urea functions are bonded and the aromatic rings are stacked upon each other. Preliminary modeling studies show that helical assemblies in which the urea (resp. amide) functions are preferentially connected to the urea (resp. amide) functions, as represented in Figures 3b and S3,[27] constitute a possible structural arrangement of the BUBA monomers. Other arrangements are probably possible, but whatever their precise connections, amide and urea groups in BUBA monomers are compatible and both stabilize the helical assemblies through hydrogen bonding.

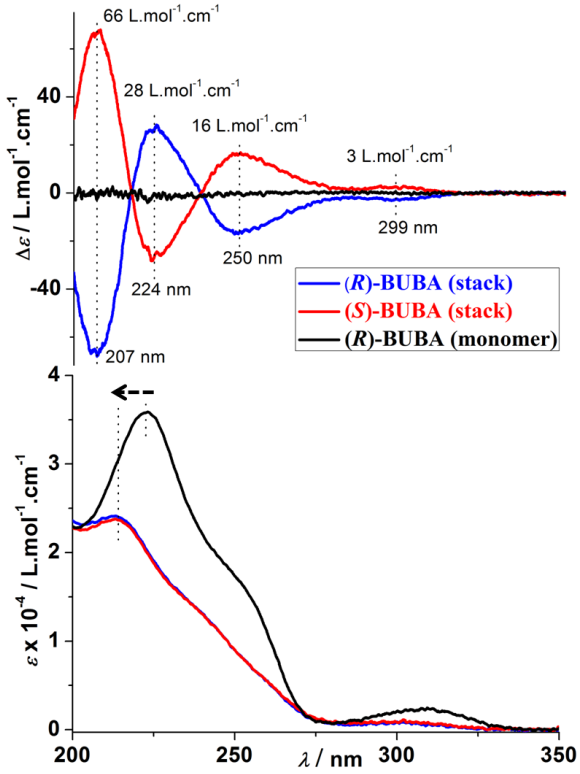

Figure 4 CD (Top) and UV-Vis absorption spectra (Bottom) of **(*R*)-BUBA** and **(*S*)-BUBA** in the assembled state (0.2 mM, DHN, 293 K) and of **(*R*)-BUBA** in the dissociated state (0.2 mM, EtOH, 293 K).

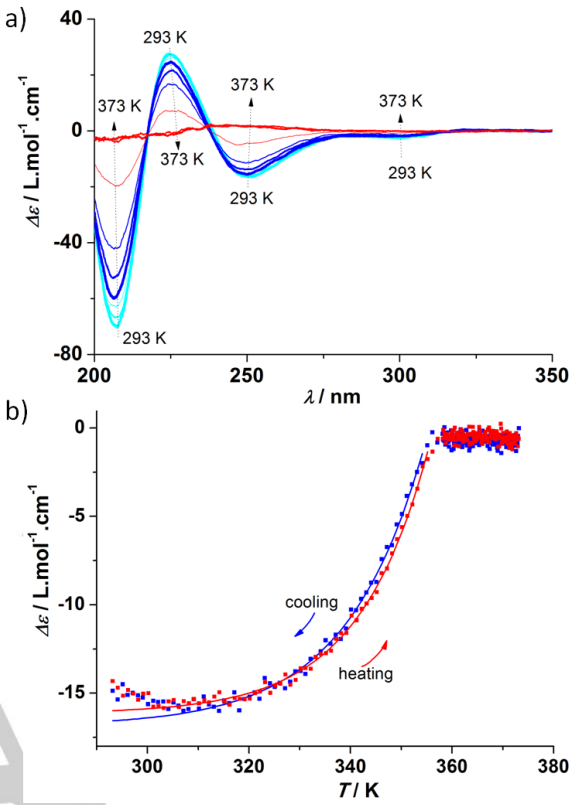

Figure 5 (a) CD spectra of **(*R*)-BUBA** from 293 K to 373 K in the heating cycle (0.2 mM, DHN), one spectrum recorded every 10 K. (b) CD cooling (■) and heating (■) curves of **(*R*)-BUBA** (0.2 mM, DHN, λ =250 nm), between 293 K and 373 K, cooling and heating rate =0.3 K.min^{-1}. The curves have been fitted with the nucleation-growth model.[31] It requires both the nucleation and elongation regimes to be fitted by two independent equations. For sake of clarity, only the fit of the elongation regime is shown**.** The decreasing of the CD values at the lower temperatures is attributed to partial precipitation occurring under these conditions.[18b]

Thermodynamic parameters of self-assembly

In the following parts, the assembly properties of BUBA monomers will be probed by several techniques and compared to those of BTA analogues of Chart 1. Spectroscopic analyses of solutions of these BTAs in toluene (Fig. 3a) and in DHN (Fig. S4) are fingerprint of the presence of very long hydrogen-bonded helices with the structure represented in Chart 1.[23a, 23c, 30] The (*rac*)-2-ethylhexyl moiety does not prevent the formation of homochiral self-assemblies, left-handed and right-handed for **(*S*)-BTA** and **(*R*)-BTA**, respectively (Fig. S4).

CD analyses of a 0.2 mM solution of **(*R*)-BUBA** in DHN show a gradual decrease of the intensity of the CD signals upon heating (Fig. 5a). The spectra obtained at 293 K and 373 K are diagnostic of the polymer and the monomer, respectively. The self-assembly process can thus be precisely probed by monitoring the CD signal at a given wavelength (Fig. 5b). The CD cooling and heating curves of **(*R*)-BUBA** have been recorded at 0.3 K.min^{-1}, a sufficiently slow rate to ensure that the assembly process is under thermodynamic equilibrium.

Firstly, the self-assembly process is fully reversible since the transitions in the cooling and heating cycles have the same amplitude. Secondly, both transitions are nonsigmoidal which implies a cooperative aggregation process of **(*R*)-BUBA** monomers in DHN. The cooperative aggregation mode of BTA monomers in organic solvents has previously been quantified by the nucleation-growth model developed by van der Schoot and co-workers,[31] and the same model has thus been applied to fit the CD cooling and heating curves of **(*R*)-BUBA** (Fig. 5b) and **(*S*)-BTA** (Fig. S5) in DHN. The extracted parameters are the dimensionless equilibrium constant K_a (activation of the monomer) and the enthalpy release upon elongation (h_e) at the elongation temperature (T_e). These values are compiled in Table 1.

Table 1 Thermodynamic parameters for the self-assembly of 0.2 mM solutions of **(*R*)-BUBA** and **(*S*)-BTA** in DHN, determined by applying the nucleation-growth model to the CD cooling and heating curves**.**

monomers	data	T_e /K	h_e / kJ.mol^{-1}	K_a
(*R*)-BUBA	CD (cooling)	354.9	−68.2	10^{-5}
	CD (heating)	355.8	−76.1	10^{-5}
(*S*)-BTA	CD (cooling)	374.7	−53.7	10^{-4}
	CD (heating)	373.8	−60.2	10^{-4}

We first comment on the thermodynamic data obtained for **(*S*)-BTA**. The average enthalpy of elongation obtained from the CD

measurements, $\overline{h_e}$ =-57 kJ.mol^{-1}, is consistent with the value obtained for a range of structurally-similar BTA monomers, including ^{octyl}**(*S*)-BTA** (Chart 1).[23a] This value is expected to be concentration/temperature independent and is thus characteristic of the enthalpically-driven assembly of the BTA monomers into the threefold hydrogen-bonded helix. The value of K_a must be interpreted cautiously since it is concentration and temperature dependent.[23a, 32] The equilibrium constant determined for **(*S*)-BTA** at 0.2 mM, K_a =10^{-4}, is more than one order of magnitude higher than that reported for ^{octyl}**(*S*)-BTA** (K_a <10^{-5}, c =0.05 mM)[23c] but is close to the value obtained for achiral BTA (c =0.05 mM).[32] The lower cooperativity of **(*S*)-BTA** compared its analogues is probably due to the presence of three branched side chains connected to the central BTA core and/or the presence of two stereoisomers which (slightly) weakens the strength of the hydrogen-bonding (HB) interactions.[33]

The average thermodynamic parameters obtained by fitting the CD cooling and heating curves of **(*R*)-BUBA** are: $\overline{T_e}$ =355 K, $\overline{h_e}$ =-72 kJ.mol^{-1} and $\overline{K_a}$ =10^{-5}. The higher absolute value of the elongation enthalpy for **(*R*)-BUBA** compared to **(*S*)-BTA** (|Δh_e| =15 kJ.mol^{-1}) probably stems from the additional hydrogen bond donor provided by the urea group. Despite the higher strength of its HB network, **(*R*)-BUBA** assemblies are slightly weaker than those of **(*S*)-BTA** as indicated by the lower T_e value (ΔT_e =-19 K). Therefore, the energetic gain from the enthalpy term is over compensated by an entropic cost, possibly due to a higher conformational order (more internal order) of the BUBA monomers within their helical self-assemblies.

The determined K_a value clearly reveals that polymerization of **(*R*)-BUBA** monomers proceeds with a good level of cooperativity and thus corroborates the formation of very long assemblies in solution. Although the values of K_a are determined at slightly different temperatures, the significant different values obtained show that BUBA assemblies are more cooperative than BTA. It is also supported by overlaying the CD cooling curves of **(*R*)-BUBA** and **(*S*)-BTA** since the change in CD intensity at T_e is clearly more abrupt in the former case (Fig. S6).

Chirality amplification properties

Chirality amplification is achieved when the main chain chirality of polymers is controlled by a small amount of chiral monomers (sergeant) combined with achiral ones (soldier) or by a small bias in the optically purity of a mixture of enantiomerically-related monomers.[11a, 34] The former phenomenon is referred to as the sergeants-and-soldiers (S&S) effect and the latter as the majority-rules (MR) principle. Cooperative assembly of monomers, notably when governed by hydrogen-bonding interactions, generates supramolecular polymers with strong chirality amplification properties. Previous studies have demonstrated the possibility of preparing homochiral BTA helices with sergeants-and-soldiers mixtures or scalemic mixtures of BTA enantiomers.[23b, 30a, 32, 35] Chirality amplification in helical supramolecular polymers has been modelled by assuming energy penalties for the inversion of handedness of the stacks (helix reversal penalty, HRP) and for the incorporation of a monomer in a stack of its unpreferred helicity (mismatch penalty, MMP).[36] Only a few studies have addressed the

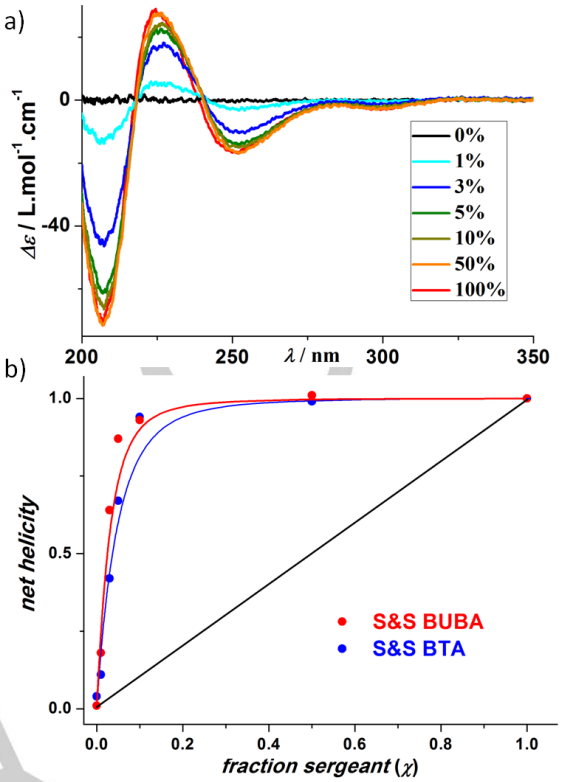

Figure 6 (a) CD spectra of the sergeants-and-soldiers type experiments obtained by mixing solutions of **(*R*)-BUBA** and **(*rac*)-BUBA** at 293 K (c_{tot} =0.2 mM, DHN). (b) Net helicity as a function of the fraction of sergeant obtained from CD mixtures of **(*R*)-BUBA** and **(*rac*)-BUBA** or of **(*S*)-BTA** and **(*rac*)-BTA** at 293 K (c_{tot} =0.2 mM, DHN). The net helicity is obtained by dividing the molar CD value at λ =207 nm (for BUBA) and at λ =225 nm (for BTA) of the S&S mixtures by the molar CD value of the pure sergeant. For each type of monomers, the data of the S&S and MR experiments have been fitted (blue and red solid lines) simultaneously following the procedures described by Smulders et al.[35] (for S&S) and by van Gestel[36b] (for MR). Please see the excel spreadsheet in the Supporting Material of this paper for all the details of the calculation. The result of the fit is indicated in the caption of Fig. 7. The black solid line represents the fate of net helicity in absence of chirality amplification.

correlation between the structure of the monomers and the extent of chirality amplification in the resulting polymer assemblies.[35, 37] As both BUBA and BTA monomers associate in a cooperative manner (*vide supra*), it makes it possible to probe the influence of the urea function on the induction and amplification of chirality in the related hydrogen-bonded helices.

We have first performed typical sergeants-and-soldiers experiments except that in our case the soldier is racemic instead of achiral. CD spectra of mixtures of **(*R*)-BUBA** and **(*rac*)-BUBA** (c_{tot} = 0.2 mM) in DHN differ by their intensity, not by their shape, which suggest that the sergeant and the soldier adopt the same conformation in the helical stacks (Fig. 6a). The same holds true for S&S mixtures between **(*S*)-BTA** and **(*rac*)-BTA** (Fig. S7a). The net helicity, *i.e.* the ratio between left-handed and right-handed fragments in the one-dimensional helical stacks, is plotted as a function of the fraction of sergeants for BUBA and BTA mixtures (Fig. 6b). Both S&S type supramolecular polymers exhibit chirality amplification properties.

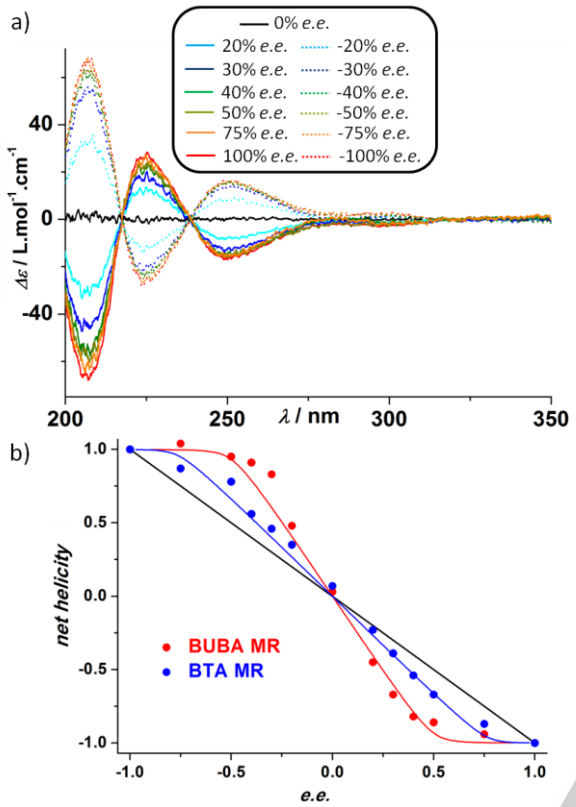

Figure 7 (a) CD spectra of the majority-rules type experiments obtained by mixing solutions of **(*R*)-BUBA** and **(*S*)-BUBA** at 293 K (c_{tot} =0.2 mM, DHN). Positive (negative) *e.e.* values correspond to mixtures enantioenriched in **(*R*)-BUBA** (**(*S*)-BUBA** resp.) monomers. (b) Net helicity as a function of the *e.e.* of the monomer obtained from CD mixtures of **(*R*)-BUBA** and **(*S*)-BUBA** or of **(*R*)-BTA** and **(*S*)-BTA** at 293 K (c_{tot}=0.2 mM, DHN). The net helicity is obtained by dividing the molar CD value at λ =207 nm (for BUBA) and at λ =225 nm (for BTA) of the MR mixtures by the molar CD value of the pure monomer. For each type of monomers, the data of the S&S and MR experiments have been fitted (blue and red solid lines) simultaneously following the procedures described by Smulders et al.[35] (for S&S) and by van Gestel[36b] (for MR). Please see the excel spreadsheet in the Supporting Material of this paper for all the details of the calculation. It provides the following values: HRP =10 kJ.mol^{-1}, MMP =2.4 kJ.mol^{-1} for BUBA and HRP =8.2 kJ.mol^{-1}, MMP =4.5 kJ.mol^{-1} for BTA. The black solid line represents the fate of the net helicity in absence of chirality amplification.

For the BTA mixtures, the maximal helicity is attained for the mixture containing *ca.* 10% of sergeants. A similar level of amplification was obtained with **^{octyl}(*S*)-BTA**[35] whereas a BTA with three chiral side chains proved to be more efficient.[30a, 32] A net helicity of 0.87 and 0.67 is reached for mixtures containing 5% of BUBA and BTA soldiers, respectively, highlighting a sligthly better induction of chirality by the sergeants in the BUBA helical assemblies.

A 3:2 mixture of **(*R*)-BUBA** and **(*S*)-BUBA** monomers in DHN (c_{tot} = 0.2 mM, 20% *e.e.*) exhibits a CD signal which is *ca.* half as intense as the one of pure **(*R*)-BUBA** (Fig. 7a). This supports the strong non-linearity in the handedness of the BUBA helices as a function of the optical purity of the monomers (Fig. 7b) and is in sharp contrast with the modest amplification of chirality observed for the mixtures of **(*S*)-BTA** and **(*R*)-BTA** (Figs. 7b and S7b).

A more precise determination of the extent of chirality amplification operating in BUBA and BTA helices is gleaned by simultaneously fitting the S&S and MR experiments for each platform following the procedures described by Smulders et al.[35] (for S&S) and by van Gestel[36b] (for MR). For the BTA platform, the HRP (8.2 kJ.mol^{-1}) and MMP (4.5 kJ.mol^{-1}) values deduced from the fits are lower and higher, respectively, to that reported in the literature for **^{octyl}(*S*)-BTA** in methylcyclohexane.[35] This is consistent with the modest degree of chirality amplification exhibited by this set of BTA helices in both S&S and MR experiments. This also connects well with the lower extent of cooperativity observed during their supramolecular polymerization (*vide supra*). We presume that the branched nature of the side chain, the presence of racemic centres in the side chains (instead of achiral or chiral ones) and/or subtle solvent effects explain the mitigated chirality amplification ability of the BTA helices investigated in this study.

The better chirality amplification of the BUBA relatively to the BTA platform is reflected by its higher HRP (10 kJ.mol^{-1}) and lower MMP (2.4 kJ.mol^{-1}) values. The mutation of a single amide function by a urea one modifies the intermolecular non-covalent network which thereby remarkably affects the energy penalties. We presume that the higher strength of the hydrogen-bond network in BUBA stacks, as deduced from the elongation enthalpy value, is responsible for the increase of the HRP which in turn lower the MMP since the two values are interconnected for a given supramolecular platform.[23b]

Mixing BUBA and BTA stacks

Combining monomers possessing different but compatible units appears as an attractive approach to generate complex architectures or co-assemblies with improved properties.[38] Previous studies related the formation of co-assemblies upon mixing C_3-symmetric monomers such as C=O-centred BTA and nitrogen-centred BTA monomers[37a] or C=O-centred BTA and benzene-1,3,5-trisurea monomers,[22] even though in the latter case segregation into single-component stacks quickly occurs after mixing. Since both BUBA and BTA self-assemble through a cooperative pathway (*vide supra*), it is interesting to probe the possibility of lowering the symmetry of BTA helices by incorporation of BUBA monomers.

Mixtures of **(*R*)-BUBA** and **(*rac*)-BTA** monomers in DHN were analyzed by CD spectroscopy (c_{tot} =0.2 mM). Firstly, the formation of copolymers was confirmed by comparing the experimental CD spectra with those simulated for a combination of the homopolymers (see Fig. 8a for the mixture containing 30% of **(*R*)-BUBA**). The much higher intensity of the experimental CD curve compared to the simulated one indicates that both co-assembly and strong chirality amplification occur. This conclusion qualitatively holds for fractions of **(*R*)-BUBA** in the mixture below 60% (Fig. S8). The compatibility between the urea and the amide functions thus prevents segregation. Interestingly, virtually identical CD spectra are obtained, shortly after mixing the preassembled homopolymers at 293 K and by slowly cooling a mixture of the monomers from 383 K down to 293 K (Fig. 8a). Thus, different pathways lead to the same co-assemblies and

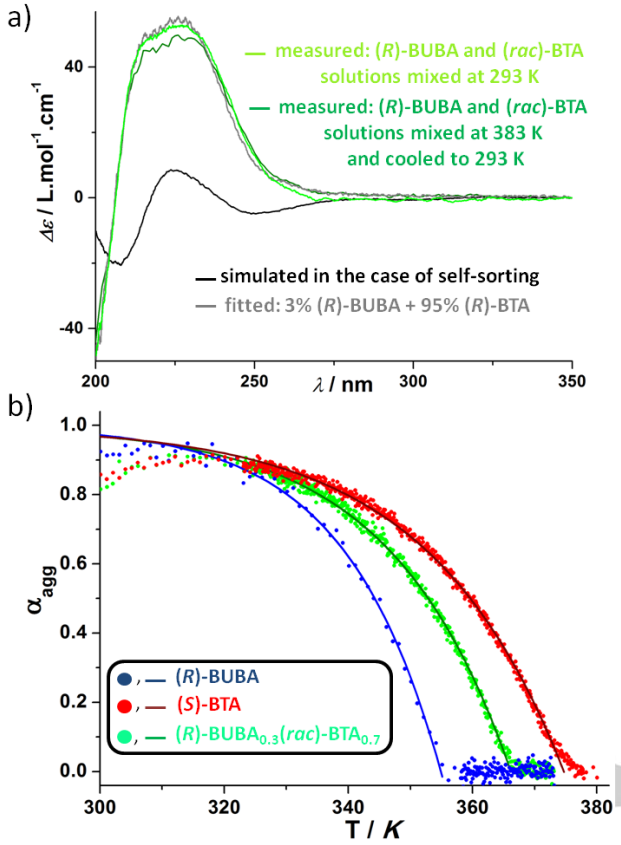

Figure 8 (a) CD spectra for the mixture of **(*R*)-BUBA** and **(*rac*)-BTA** (3:7) prepared by two different methods (c_{tot} =0.2 mM, DHN). The experimental spectra are shown together with the fitted spectrum (see Fig. S8 and the text for more details) and the simulated CD curve for segregated stacks (no co-assembly). (b) CD cooling curve of **(*R*)-BUBA**/**(*rac*)-BTA** 3/7 mixture (c_{tot} = 0.2 mM, DHN, λ =225 nm), between 293 K and 383 K, cooling and heating rate =0.3 K.min^{-1}. The curves have been fitted with the nucleation-growth model.[31] Result of the fit: T_e =366 K, h_e =−58 kJ.mol^{-1}, K_a =10^{-5}. For the sake of comparison, the CD curves of pure **(*R*)-BUBA** and **(*S*)-BTA** are also shown.

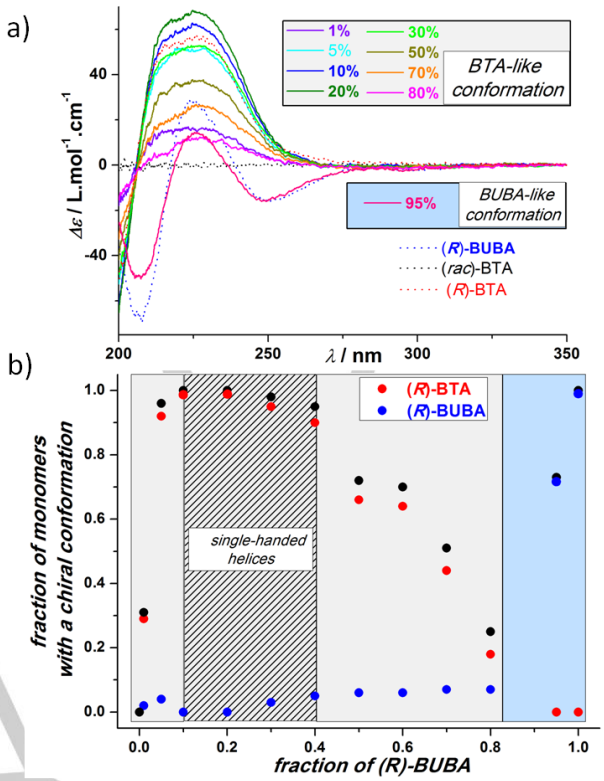

Figure 9 (a) CD spectra of mixtures of **(*R*)-BUBA** (0-100%) and **(*rac*)-BTA** at 293 K (c_{tot} =0.2 mM, DHN). In the caption, the mixtures are sorted according to the conformation preferentially adopted by the co-assemblies as determined by fitting the CD curves (Figs. 8 and S8). (b) Fraction of monomers with a chiral conformation in the co-assemblies as a function of the fraction of **(*R*)-BUBA** in the mixtures. The total fraction of chiral monomers (black dots) corresponds to the sum of monomers with **(*R*)-BTA**-like (red dots) and **(*R*)-BUBA**-like (blue dots) conformations as determined by fitting the experimental CD curves of the different mixtures (Fig. S8 and Table S1). The zones filled in light grey and light blue correspond to co-assemblies which preferentially adopt a BTA-like and BUBA-like conformation, respectively. The hatched area correspond to fully chirally-amplified co-assemblies.

the dynamic nature of BTA and BUBA assemblies allows rapid equilibration of the composition and favours the formation of the copolymers. Further information on the co-assembly process is disclosed by the CD cooling curve of the mixture containing 30% of **(*R*)-BUBA** (Fig. 8b). Co-polymerization occurs cooperatively with a T_e value of 366 K, *i.e.* higher than for **(*R*)-BUBA** homopolymer and close to the one found for **(*S*)-BTA** homopolymer. Importantly, the presence of a single T_e value is an additional testimony of a co-assembly rather than a self-sorting process since the latter one would have exhibited two distinct transitions.

Although BUBA and BTA self-assemblies share structural similarities (*vide supra*), their strikingly different CD spectroscopic signatures infer that they do not adopt identical conformations and this must be taken into consideration when interpreting the CD spectra of their mixtures. A closer look at the experimental CD curves at 293 K (Fig. 9a) reveals that all spectra, except the one containing 95% of **(*R*)-BUBA**, exhibit a CD signal which has a similar shape as the CD signal of **(*R*)-BTA**. From this, it can be deduced qualitatively that the **(*rac*)-BTA** units adopt preferentially the conformation of **(*R*)-BTA** helices in presence of **(*R*)-BUBA**. Fitting the CD curves can provide more quantitative information about the extent of chirality amplification and the conformation displayed by these helical co-assemblies (Figs. 8a and S8). More precisely, the experimental CD spectrum is simulated by combining the individual spectra of **(*R*)-BUBA** and **(*R*)-BTA** and their content is adjusted to minimize the difference between the simulated and experimental spectra. The good quality of the fits allows to extract the relative contribution of **(*R*)-BUBA** and **(*R*)-BTA** to the overall CD signal displayed by the co-assemblies (Table S1). The fraction of stacks adopting **(*R*)-BUBA**-like (blue dots) or **(*R*)-BTA**-like (red dots) conformations is plotted in Fig. 9b as a function of the introduced fraction of **(*R*)-BUBA** in the mixture, and the concentration of all species present (*i.e.* the speciation plot) is shown in Fig. S9.

Three characteristic zones emerge from this analysis: (i) for mixtures containing between 5% and 40% of **(*R*)-BUBA** most of the monomers adopt a chiral conformation (*i.e.* full chiral amplification occurs). Moreover, **(*R*)-BUBA** (the sergeant) imposes its helical preference, but **(*rac*)-BTA** (the soldier, which

is present in excess) imposes its conformation. (ii) In the intermediate range (from 50% to 80% **(*R*)-BUBA**) the soldier still imposes its conformation to a significant fraction of the sergeant but it also creates defects that result in a reduced chirality amplification.[39] (iii) In the range above 80% of **(*R*)-BUBA** both the helicity and the conformation are imposed by the sergeant. These results stress out the strong interaction between the monomers in the helical co-assemblies which is in striking contrast with the weak interactions between structurally-similar hydrogen-bonded monomers recently reported in the literature.[40] This also points towards an alternate or random organization of the monomers within the BUBA/BTA copolymers. Most importantly, these mixing experiments highlight the efficient incorporation of BUBA monomers into the one-dimensional helical assemblies of BTA. Thanks to chirality-amplification phenomena, 10% of BUBA "sergeants" are enough to generate single-handed co-assemblies with a BTA-like conformation. The compatibility between the urea and amide functions in the mixed aggregates also dictates the monomer interactions and this can probably be further extended to control the monomer sequences in such types of chiral supramolecular co-polymers.[40-41]

Conclusions

Compatibility between the recognition units dictates the assembly properties of disk-like molecules possessing multiple functional groups. Here, we show that *N*-substituted benzene-1-urea-3,5-biscarboxamide (BUBA) monomers, comprising one urea function and two carbon-centred amide functions connected to the same aromatic ring, form long, reversible and highly chirally-amplified helical assemblies in apolar solvents. This class of monomers provides an easy access to non C_3-symmetric supramolecular helices which are useful for the design of hierarchical assemblies, for the compartmentalization or self-assembly of polymer chains and for application-driven studies in asymmetric catalysis. Single-handed helices are obtained by self-assembly of BUBA monomers possessing chiral sides chains and more importantly by incorporating a small amount of chiral BUBA monomers in a racemic mixture of left- and right-handed benzene-1,3,5-tricarboxamide (BTA) stacks.

By comparing the structure BUBA and BTA monomers, our study also provides the influence of a single mutation on the structure and properties of the resulting supramolecular polymers. Such structure – properties relationships, notably when considering the triad: stability – mechanism of aggregation – chirality amplification, are currently lacking despite their necessity for the design of more efficient supramolecular polymer platforms. Clearly, BUBA and BTA assemblies have more similarities than differences. They both aggregate through hydrogen bonding and aromatic interactions by means of a cooperative mechanism, form long helices in solution, are reversible and their main chain helicity can be amplified. Nevertheless, the stability of BUBA assemblies is slightly lower despite the presence of an additional hydrogen bond interaction provided by the urea groups (as reflected by the higher elongation enthalpy). Conversely, BUBA self-assembly proceeds with a higher level of cooperativity and the main chain chirality of their resulting helices is more strongly amplified. It is worth to note that previous modification of the BTA structure led to mitigated properties for the resulting assemblies in term of reversibility, stability, cooperativity and chirality amplification.[22, 23d, 23e, 37a, 37b]

Ongoing work in our laboratory is focused on better understanding of the BUBA assemblies at the molecular level and notably the position of the urea groups, the possibility of controlling the monomer sequence in BUBA co-assemblies and the implementation of BUBA assemblies in asymmetric catalysis.

Experimental Section

Materials: *N*,*N*',*N*''-tris(2-ethylhexyl)benzene-1,3,5-tricarboxamide (**(*rac*)-BTA**),[25] 1-(4-Tolyl)-3-(2-EthylHexyl)-Urea (**4TEHU**),[24] *N*-(2-EthylHexyl)BenzenecarboxAmide (**EHBA**),[42] and 5-methoxycarbonyl-benzene-1,3-dicarboxylic acid[16] were prepared by following or adapting published procedures. *N*-(3-dimethylaminopropyl)-*N*'-ethylcarbodiimide hydrochloride (EDC·HCl) was purchased from Fluorochem. 4-(Dimethylamino)pyridine (DMAP), *N*,*N*-diisopropylethylamine (DIEA), dimethyl 5-aminoisophthalate, (*S*)-2-octylamine, (*R*)-2-octylamine, 2-ethylhexylamine, LiOH and triphosgene were purchased from Sigma-Aldrich. All the chemicals were used as received. C_7D_8 was bought from Eurisotop and used without further purification. Decahydronaphthalene (DHN), mixture of *cis* and *trans* isomers (purity≥99%), was bought from Sigma-Aldrich and used without further purification. Dried toluene and dichloromethane (DCM) were obtained from a Solvent Purification System (SPS).

Methods: NMR spectra were recorded on a Bruker Avance 400 spectrometer and calibrated to the residual solvent peak: dmso-d_6 (^{1}H: 2.50 ppm; ^{13}C: 39.52 ppm). Peaks are reported with their corresponding multiplicity (s: singlet; br s: broad singlet, d: doublet, t: triplet; sept.: septuplet, m: multiplet) coupling constants and integration.

Exact mass measurements (HRMS) were obtained on TQ R30-10 HRMS spectrometer by ESI^+ ionization and are reported in *m/z* for the major signal.

Fourier-Transform Infrared (FT-IR) measurements were performed on a Nicolet iS10 spectrometer. Spectra for toluene or DHN solutions were measured in 0.02 cm pathlength CaF_2 cells at 293 K and were corrected for air, solvent and cell absorption. Spectra for solids were recorded by reflection on a Ge probe (ATR-FTIR) and the main peaks were reported (m: medium, s: strong, w: wide).

Circular dichroism (CD) measurements were performed on a Jasco J-1500 spectrometer equipped with a Peltier thermostated cell holder and Xe laser. Data were recorded with the following parameters: 50 nm.min^{-1} sweep rate, 0.05 nm data pitch, 2.0 nm bandwidth, and between 350 and 200 nm. A 1 mm quartz cell was used. DHN and cell contributions at the same temperature were subtracted from the obtained signals. For all samples, LD contribution was negligible (ΔLD < 0.005 dOD) and the shape of the CD signal was independent of the orientation of the quartz cell. Molar CD values are reported in L.mol^{-1}.cm^{-1} and are expressed as follows: $\Delta\varepsilon=\theta/(32980\times l\times c)$ where θ is the measured ellipticity (mdeg), l is the optical pathlength in cm, and c is the concentration in mol.L^{-1}. For VT-CD experiments, the temperature was controlled with a Peltier thermostated cell holder, one spectrum was recorded every 10 K between 293 K and 373 K and the heating and cooling rates were set to 1K.min^{-1}. The ellipticity was also recorded at 225 nm (for BTA monomers) and 250 nm (for BUBA monomers) and the heating and cooling rates were set to 1K.min^{-1}.

UV-Vis absorption spectra were extracted from CD analyses on each of the above samples and obtained after correction of the absorption of air, solvent, and cell contribution at the same temperature.

Small-angle neutron scattering (SANS) measurements were made at the LLB (Saclay, France) on the PA20 instrument, at three distance-wavelength combinations to cover the 2.4×10^{-3} to 0.46 Å q^{-1} range, where the scattering vector q is defined as usual, assuming elastic scattering, as $q=(4\pi/\lambda)\sin(\theta/2)$, where θ is the angle between incident and scattered beam. Data were corrected for the empty cell signal and the solute and solvent incoherent background. A light water standard was used to normalize the scattered intensities to cm^{-1} units. The data was fitted with the DANSE software SasView. The number *n* of molecule in

the cross-section can be derived from n_L (the number of molecule per unit length) by assuming an average intermolecular distance of 3.62 Å, which is the usual spacing between aromatic rings in BTA helical assemblies.

Preparation of the solutions of BUBA and BTA homopolymers: Desired amounts of monomer and solvent were introduced in a vial sealed with a PTFE-coated cap to avoid contamination from leaching plasticizer, and briefly heated up to solvent boiling point to ensure dissolution. After cooling down to room temperature, the solutions were quickly analyzed. Preparation of S&S, MR and BUBA/BTA mixtures: Stock solutions of the pure monomers were mixed in the desired amount, briefly heated up to solvent boiling point, cooled down to room temperature and quickly analyzed.

Synthesis of BUBA precursors. Synthesis of 3,5-dimethyl-1-(2-ethylhexyl urea) benzoate, (**1**): In an oven-dried Schlenk flask, a solution of dimethyl 5-aminoisophthalate (1.0 g, 4.78 mmol, 1.0 equiv.) and DIEA (678 mg, 5.26 mmol 1.1 equiv.) in DCM (40 mL) was added with a syringe pump (10 mL/h) to a solution of triphosgene (0.47 g, 1.57 mmol, 0.33 equiv.) in DCM (10 mL). The solution was stirred 5 additional minutes and 2-ethylhexylamine (678 mg, 5.26 mmol 1.1 equiv.) and DIEA (678 mg, 5.26 mmol, 1.1 equiv.) were added to the solution. The reaction mixture was stirred overnight. The volatiles were evaporated under vacuum and the crude product was taken up in AcOEt and washed successively with an aqueous solution of HCl (2 M), an aqueous solution of NaOH (1 M) and brine. The organic phase was dried over $MgSO_4$ and evaporated under vacuum to yield **1** as a colourless solid which was used for the next step without further purification (1.31 g, 75% yield). ^{1}H NMR (dmso-d_6): δ (ppm) = 8.94 (s, 1H), 8.25 (m, 2H), 8.00 (m, 1H), 6.17 (t, 1H, ^3J=5.8 Hz), 3.87 (s, 6H), 3.05 (m, 2H), 1.55-1.05 (m, 9H), 0.96-0.77 (m, 6H). ^{13}C{^{1}H} NMR (dmso-d_6): δ (ppm) = 165.5, 155.0, 141.6, 130.5, 121.9, 121.8, 52.4, 30.4, 28.4, 23.6, 22.5, 13.9, 10.7. FT-IR (ATR, cm^{-1}): 643 (m), 756 (m), 990 (w), 1122 (m), 1244 (s), 1348 (m), 1442 (m), 1555 (s), 1640 (s), 1724 (s), 2937 (w), 3303 (w). HRMS (ESI, *m/z*): Calculated for $C_{19}H_{28}N_2O_5Na$, [M+ Na]$^+$: 387.1890, found: 387.1890.

Synthesis of {1-(2-ethylhexyl urea)}-3,5-benzoic diacid, (**2**): Compound **1** (1.0 g, 2.58 mmol, 1.0 equiv.) was dissolved in methanol (100 mL). LiOH (197 mg, 8.26 mmol, 3.2 equiv.) and H_2O (1.0 g) were added and the mixture was heated to 55 °C overnight. Then, 100 mL of water and 100 mL of an aqueous solution of HCl (1 M) were added successively. A white powder precipitated which was isolated by filtration, washed with H_2O, and dried over P_2O_5 under vacuum to give **2** as a colourless solid (0.88 g, 95% yield). ^{1}H NMR (dmso-d_6): δ (ppm) =13.09 (s, 2H), 8.83 (s, 1H), 8.20 (m, 2H), 8.00 (m, 1H), 6.17 (t, 1H, ^3J=5.8 Hz), 3.05 (m, 2H), 1.55-1.05 (m, 9H), 0.96-0.77 (m, 6H). ^{13}C{^{1}H} NMR (dmso-d_6): δ (ppm) = 166.7, 155.1, 141.3, 131.6, 122.4, 122.0, 41.7, 30,5, 28.5, 23.7, 22.6, 14.0, 10.8. FT-IR (ATR, cm^{-1}): 638 (m),758 (m), 990 (m), 1122 (m), 1231 (s), 1348 (m), 1437 (m), 1555 (s), 1640 (s) , 1730 (s), 2927 (w), 3296 (w). HRMS (ESI, *m/z*): Calculated for $C_{17}H_{24}N_2O_5Na$, [M+ Na]$^+$:359.1577, found :359.1576.

General procedure for the synthesis of BUBA monomers: Compound **2** (1.0 equiv.) was dissolved in THF, and DMAP (3.4 equiv.), the desired amine (3.0 equiv.), and EDC·HCl (3.4 equiv.) were added successively. The solution was refluxed for 2 days. Then, THF was removed, the crude solid was dissolved in CH_2Cl_2 and the solution was washed with an aqueous solution of HCl (1 M), an aqueous solution of $NaHCO_3$ (1 M) and with brine successively. The organic phase was dried over $MgSO_4$ filtered, and purified by flash column chromatography (SiO_2, CH_2Cl_2/AcOEt). The obtained solids were recrystallized from MeCN yielding pure BUBA monomers as colourless solids.

***(S)*-BUBA** (with (*S*)-2-octylamine, crystalline solid, 1.0 g, 70% yield): ^{1}H NMR (dmso-d_6): δ (ppm) =8.62 (s, 1H), 8.15 (d, ^3J=8.2 Hz, 2H), 7.87 (br s, 2H), 7.69 (br s, 1H), 6.13 (t, ^3J=5.5 Hz, 1H), 3.98 (sept., ^3J=6.5 Hz, 2H), 3.14-2.97 (m, 2H), 1.67-1.18 (m, 29H), 1.12 (d, ^3J = 6.5 Hz, 6H), 1.02-0.83 (m, 12H). ^{13}C{^{1}H} NMR (dmso-d_6): δ (ppm) = 165.7, 155.1, 140.4, 135.9, 118.7, 118.4, 44.9, 41.6, 35.9, 31.2, 30.4, 28.6, 28.4, 25.8, 23.7, 22.5, 22.0, 20.7, 13.9, 10.8. FT-IR (ATR, cm^{-1}): 699 (m), 1225 (m), 1263 (m), 1451 (m),1545 (s), 1620 (m), 2927 (m), 3271 (m), 3345 (s). HRMS (ESI, *m/z*): Calculated for $C_{33}H_{58}N_4O_3Na$, [M+ Na]$^+$: 581.4401, found: 581.4403.

***(R)*-BUBA** (with (*R*)-2-octylamine, crystalline solid, 1.5 g, 78% yield): Spectroscopic data are identical to **(*S*)-BUBA**. HRMS (ESI, *m/z*): Calculated for $C_{33}H_{58}N_4O_3Na$, [M+ Na]$^+$: 581.4401, found: 581.4400.

***(rac)*-BUBA** (with 2-ethylhexylamine, amorphous solid, 2.0 g, 71% yield): ^{1}H NMR (dmso-d_6): δ (ppm) =8.61 (s, 1H), 8.33 (t, ^3J=5.3 Hz, 2H), 7.90 (br s, 2H), 7.72 (br s, 1H), 6.15 (t, ^3J=5.4 Hz, 1H), 3.18 (t, ^3J=5.9 Hz, 4H), 3.11-2.98 (m, 2H), 1.62-1.47 (m, 2H), 1.45-1.14 (m, 25H), 0.95-0.79 (m, 18H). ^{13}C{^{1}H} NMR (dmso-d_6): δ (ppm) = 165.9, 155.1, 140.5, 135.8, 118.4, 118.3, 42.4, 41.6, 30.5, 30.4, 28.4, 28.3, 23.7, 22.5, 13.9, 10.5. FT-IR (ATR, cm^{-1}): 689 (m), 1228 (m), 1271 (m), 1452 (m), 1535 (s), 1638 (m), 2924 (m), 3302 (m). HRMS (ESI, *m/z*): Calculated for $C_{33}H_{58}N_4O_3Na$, [M+ Na]$^+$: 581.4401, found: 581.4402.

Synthesis of BTA precursors.

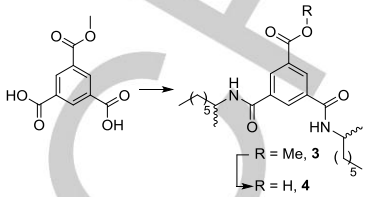

Synthesis of methyl 3,5-bis-(1*S*)-(1-methyl-heptylcarbonyl)-1-methyl-benzoate (**3*S***): 5-methoxycarbonyl-benzene-1,3-dicarboxylic acid[16] (2.48 g, 11.0 mmol, 1.0 equiv.) was dissolved in THF (100 mL), then DMAP (4.60 g, 37.6 mmol, 3.4 equiv.), (*S*)-2-octylamine (4.29 g, 33.2 mmol, 3 equiv.) and EDC·HCl (7.21 g, 37.6 mmol, 3.4 equiv.) were added successively. The solution was reflux for 2 days. Then, THF was evaporated, the crude solid was dissolved in CH_2Cl_2, washed with an aqueous solution of HCl (1M), an aqueous solution of $NaHCO_3$ (10%) and with brine successively. The organic phase was dried over $MgSO_4$, filtered and purified by flash column chromatography (SiO_2, CH_2Cl_2/AcOEt=92/8) yielding **3*S*** as a colourless solid. (1.9 g, 51% yield). ^{1}H NMR (dmso-d_6): δ (ppm) =8.70-8.22 (m, 5H), 4.14-3.96 (m, 2H), 3.92 (s, 3H), 1.70-103 (m, 26H), 0.95-0.67 (m, 6H). ^{13}C{^{1}H} NMR (dmso-d_6): δ (ppm) =166.5, 164.2, 135.6, 130.8, 129.9, 129.7, 52.4, 45.0, 31.2, 28.5, 25.8, 22.0, 20.6, 13.8. FT-IR (ATR, cm^{-1}): 708 (s), 1265 (s), 1632 (s), 1731 (s), 2855 (w), 2925 (m), 3242 (m). HRMS (ESI, *m/z*): Calculated for $C_{26}H_{42}N_2O_4Na$, [M+ Na]$^+$:469.3037, found : 469.3036.

Compound **3*R*** (1.4 g, 37% yield) was obtained following the same procedure with (*R*)-2-octylamine and spectroscopic data are identical to **3*S***.

Synthesis of 3,5-bis-(1*S*)-(1-methyl-heptylcarbonyl)-1-benzoic acid (**4*S***): compound **3*S*** (1.9 g, 5.6 mmol, 1 equiv.) was dissolved in methanol (150 mL). LiOH (216 mg, 9 mmol, 1.6 equiv.) and H_2O (3 mL) were added and the mixture was heated to 55°C overnight. Then, 500 mL of water was added and the solution was acidified until pH≈1. A white powder precipitated which was isolated by filtration, washed with H_2O and dried over P_2O_5 under vacuum yielding **4*S*** as a colourless solid (1.6 g, 90% yield). ^{1}H NMR (dmso-d_6): δ (ppm) =8.89-7.86 (m, 5H), 4.32-3.85 (m, 2H), 1.70-1.03 (m, 26H), 0.95-0.67 (m, 6H). ^{13}C{^{1}H} NMR (dmso-d_6): δ (ppm) =166.5, 164.2, 135.7, 130.8, 129.9, 129.7, 45.0, 39.5, 35.8, 31.2, 28.5, 25.8, 22.0, 20.6, 13.8. FT-IR (ATR, cm^{-1}): 669 (s), 689 (s), 989 (s), 1021 (s), 1256 (s), 1443 (w), 1538 (s), 1640 (s), 1703 (w), 2853 (w), 2926 (m), 2960 (w), 3283 (m). HRMS (ESI, *m/z*): Calculated for $C_{25}H_{40}N_2O_4Na$, [M+ Na]$^+$: 455.2880, found: 455.2879.

Compound **4*R*** (1.5 g, 84% yield) was obtained following the same procedure with ***3R*** and spectroscopic data are identical to **4*S***.

General procedure for the synthesis of BTA monomers: Compound **4** (1.0 equiv.) was dissolved in THF and DMAP (1.7 equiv.), 2-ethylhexylamine (1.5 equiv.), and EDC·HCl (1.7 equiv.) were added successively. The solution was refluxed for 2 days. Then, THF was removed, the crude solid was dissolved in CH_2Cl_2 and the solution was washed with water. The organic phase was dried over $MgSO_4$, filtered and purified by flash column chromatography (SiO_2, CH_2Cl_2/AcOEt). The obtained solids were recrystallized from MeCN yielding pure BTA monomers as colourless amorphous solids.

(S)*-BTA** (with **4*S, 1.0 g, 57% yield): ^{1}H NMR (dmso-d_6): δ (ppm) =8.58 (t, ^3J=5.5 Hz, 1H), 8.40 (d, ^3J=8.3 Hz, 2H), 8.33 (s, 3H), 4.02 (sept., ^3J=7.0 Hz, 2H), 3.21 (t, ^3J = 6.3 Hz, 2H), 1.65-1.41 (m, 4H), 1.39-1.20 (m, 25H), 1.15 (d, ^3J =6.6 Hz, 6H), 0.95-0.78 (m, 12H). ^{13}C{^{1}H} NMR (dmso-d_6): δ (ppm) =165.7, 165.0, 135.3, 135.1, 128.4, 128.3, 45.1, 42.5, 35.9, 31.2, 30.4, 28.6, 28.3, 25.8, 23.7, 22.5, 22.0, 20.7, 13.9, 13.8, 10.6. FT-IR (ATR, cm^{-1}): 667 (s), 691 (s), 987 (s), 1024 (s), 1254 (s), 1537 (s), 1639 (s), 1706 (m), 2854 (w), 2932 (m), 3287 (m). HRMS (ESI, *m/z*): Calculated for $C_{33}H_{57}N_3O_3Na$, [M+ Na]$^+$: 566.4292, found : 566.4291.

(R)*-BTA**: (with **4*R, 1.5 g, 50% yield): HRMS (ESI, *m/z*): Calculated $C_{33}H_{57}N_3O_3Na$, [M+ Na]$^+$: 566.4292, found: 566.4292.

Acknowledgements

This work was supported by the China Scholarship Council (CSC, PhD grant of Y.L.). Jacques Jestin (LLB, Saclay) is acknowledged for assistance with SANS experiment. B.G.A. thanks the Sao Paulo Research Foundation (FAPESP, Sao Paulo, Brazil) for a fellowship (2014/04515-8).

Keywords: supramolecular chirality, functional compatibility, helical assemblies, cooperativity, chirality amplification, co-assembly.

References

[1] a) M. Liu, L. Zhang, T. Wang, *Chem. Rev.* **2015**, *115*, 7304-7397; b) E. Yashima, N. Ousaka, D. Taura, K. Shimomura, T. Ikai, K. Maeda, *Chem. Rev.* **2016**, *116*, 13752-13990.

[2] A. J. Boersma, R. P. Megens, B. L. Feringa, G. Roelfes, *Chem. Soc. Rev.* **2010**, *39*, 2083-2092.

[3] K. Kodama, Y. Kobayashi, K. Saigo, *Chem. Eur. J.* **2007**, *13*, 2144-2152.

[4] S. H. Jung, J. Jeon, H. Kim, J. Jaworski, J. H. Jung, *J. Am. Chem. Soc.* **2014**, *136*, 6446-6452.

[5] M. Leyendecker, N. C. Meyer, C. M. Thiele, *Angew. Chem. Int . Ed.* **2017**, *56*, 11471-11474.

[6] a) C. F. C. Fitié, W. S. C. Roelofs, M. Kemerink, R. P. Sijbesma, *J. Am. Chem. Soc.* **2010**, *132*, 6892-6893; b) C. F. C. Fitié, W. S. C. Roelofs, P. C. M. M. Magusin, M. Wübbenhorst, M. Kemerink, R. P. Sijbesma, *J. Phys. Chem. B* **2012**, *116*, 3928-3937; c) I. Urbanaviciute, X. Meng, T. D. Cornelissen, A. V. Gorbunov, S. Bhattacharjee, R. P. Sijbesma, M. Kemerink, *Adv. Electron. Mater.* **2017**, *3*, 1600530.

[7] a) Z. C. Shen, T. Y. Wang, L. Shi, Z. Y. Tang, M. H. Liu, *Chem. Sci.* **2015**, *6*, 4267-4272; b) H. Wu, Y. Zhou, L. Yin, C. Hang, X. Li, H. Ågren, T. Yi, Q. Zhang, L. Zhu, *J. Am. Chem. Soc.* **2017**, *139*, 785-791; c) A. Sandeep, V. K. Praveen, K. K. Kartha, V. Karunakaran, A. Ajayaghosh, *Chem. Sci.* **2016**, *7*, 4460-4467.

[8] a) W. Mtangi, F. Tassinari, K. Vankayala, A. Vargas Jentzsch, B. Adelizzi, A. R. A. Palmans, C. Fontanesi, E. W. Meijer, R. Naaman, *J. Am. Chem. Soc.* **2017**, *139*, 2794-2798; b) T. J. Zwang, S. Hurlimann, M. G. Hill, J. K. Barton, *J. Am. Chem. Soc.* **2016**, *138*, 15551-15554.

[9] Y. Dorca, J. Matern, G. Fernández, L. Sanchez, *Isr. J. Chem.* **2019**, DOI: 10.1002/ijch.201900017.

[10] a) T. F. A. De Greef, M. M. J. Smulders, M. Wolffs, A. P. H. J. Schenning, R. P. Sijbesma, E. W. Meijer, *Chem. Rev.* **2009**, *109*, 5687-5754; b) L. L. Yang, X. X. Tan, Z. Q. Wang, X. Zhang, *Chem. Rev.* **2015**, *115*, 7196-7239.

[11] a) A. R. A. Palmans, E. W. Meijer, *Angew. Chem. Int . Ed.* **2007**, *46*, 8948-8968; b) F. Ishiwari, Y. Shoji, T. Fukushima, *Chem. Sci.* **2018**, *9*, 2028-2041; c) Y. Dorca, E. E. Greciano, J. S. Valera, R. Gómez, L. Sánchez, *Chem. Eur. J.* **2019**, DOI: 10.1002/chem.201805577.

[12] S. Cantekin, T. F. A. de Greef, A. R. A. Palmans, *Chem. Soc. Rev.* **2012**, *41*, 6125-6137.

[13] a) M. Raynal, F. Portier, P. W. N. M. van Leeuwen, L. Bouteiller, *J. Am. Chem. Soc.* **2013**, *135*, 17687-17690; b) E. Huerta , B. van Genabeek , B. A. G. Lamers, M. M. E. Koenigs, E. W. Meijer, A. R. A. Palmans, *Chem. Eur. J.* **2015**, *21*, 3682-3690; c) L. N. Neumann, M. B. Baker, C. M. A. Leenders, I. K. Voets, R. P. M. Lafleur, A. R. A. Palmans, E. W. Meijer, *Org. Biomol. Chem.* **2015**, *13*, 7711-7719; d) A. Desmarchelier, X. Caumes, M. Raynal, A. Vidal-Ferran, P. W. N. M. van Leeuwen, L. Bouteiller, *J. Am. Chem. Soc.* **2016**, *138*, 4908-4916; e) J. M. Zimbron, X. Caumes, Y. Li, C. M. Thomas, M. Raynal, L. Bouteiller, *Angew. Chem. Int . Ed.* **2017**, *56*, 14016-14019; f) L. Yan, X. Caumes, M. Raynal, L. Bouteiller, *Chem. Commun.* **2019**, *55*, 2162-2165.

[14] P. J. M. Stals, P. A. Korevaar, M. A. J. Gillissen, T. F. A. de Greef, C. F. C. Fitié, R. P. Sijbesma, A. R. A. Palmans, E. W. Meijer, *Angew. Chem. Int . Ed.* **2012**, *51*, 11297-11301.

[15] a) T. Mes, R. van der Weegen, A. R. A. Palmans, E. W. Meijer, *Angew. Chem. Int . Ed.* **2011**, *50*, 5085-5089; b) N. Hosono, M. A. J. Gillissen, Y. C. Li, S. S. Sheiko, A. R. A. Palmans, E. W. Meijer, *J. Am. Chem. Soc.* **2013**, *135*, 501-510; c) O. Altintas, M. Artar, G. ter Huurne, I. K. Voets, A. R. A. Palmans, C. Barner-Kowollik, E. W. Meijer, *Macromolecules* **2015**, *48*, 8921-8932; d) Y. Ogura, M. Artar, A. R. A. Palmans, M. Sawamoto, E. W. Meijer, T. Terashima, *Macromolecules* **2017**, *50*, 3215-3223; e) M. L. Ślęczkowski, E. W. Meijer, A. R. A. Palmans, *Macromol. Rapid. Commun.* **2017**, *38*.

[16] J. Roosma, T. Mes, P. Leclère, A. R. A. Palmans, E. W. Meijer, *J. Am. Chem. Soc.* **2008**, *130*, 1120-1121.

[17] M. García-Iglesias, B. F. M. de Waal, I. de Feijter, A. R. A. Palmans, E. W. Meijer, *Chem. Eur. J.* **2015**, *21*, 377-385.

[18] For multi-step synthesis of non C_3-symmetric BTA and BTA related monomers see also: a) W. Zhang, D. Horoszewski, J. Decatur, C. Nuckolls, *J. Am. Chem. Soc.* **2003**, *125*, 4870-4873; b) F. García, L. Sánchez, *J. Am. Chem. Soc.* **2012**, *134*, 734-742.

[19] a) J. J. Van Gorp, J. A. J. M. Vekemans, E. W. Meijer, *Mol. Cryst. Liq. Cryst.* **2003**, *397*, 191-205; b) N. San-José, A. Gómez-Valdemoro, F. C. García, F. Serna, J. M. García, *J. Polym. Sci. A* **2007**, *45*, 4026-4036.

[20] a) Bayer, DE 2417763, **1975**; b) S. Bera, S. K. Maity, D. Haldar, *CrystEngComm* **2014**, *16*, 4834-4841.

[21] a) P. Mohan, R. Singh, M. Baba, *Biochem. Pharmacol.* **1991**, *41*, 642-646; b) M. U. Kassack, K. Braun, M. Ganso, H. Ullmann, P. Nickel, B. Boing, G. Muller, G. Lambrecht, *Eur. J. Med. Chem.* **2004**, *39*, 345-357; c) D. F. McCain, L. Wu, P. Nickel, M. U. Kassack, A. Kreimeyer, A. Gagliardi, D. C. Collins, Z. Y. Zhang, *J. Biol. Chem.* **2004**, *279*, 14713-14725; d) N. San-José, A. Gómez-Valdemoro, S. Ibeas, F. C. García, F. Serna, J. M. García, *Supramol. Chem.* **2010**, *22*, 325-338; e) D. S. Wilbur, S. I. Park, M. K. Chyan, F. Wan, D. K. Hamlin, J. Shenoi, Y. Lin, S. M. Wilbur, F. Buchegger, A. Pantelias, J. M. Pagel, O. W. Press, *Bioconjug. Chem.* **2010**, *21*, 1225-1238.

[22] J. J. van Gorp, J. A. J. M. Vekemans, E. W. Meijer, *J. Am. Chem. Soc.* **2002**, *124*, 14759-14769.

[23] a) P. J. M. Stals, M. M. J. Smulders, R. Martín-Rapún, A. R. A. Palmans, E. W. Meijer, *Chem. Eur. J.* **2009**, *15*, 2071-2080; b) M. M. J. Smulders, I. A. W. Filot, J. M. A. Leenders, P. van der Schoot, A. R. A. Palmans, A. P. H. J. Schenning, E. W. Meijer, *J. Am. Chem. Soc.* **2010**, *132*, 611-619; c) Y. Nakano, T. Hirose, P. J. M. Stals, E. W. Meijer, A. R. A. Palmans, *Chem. Sci.* **2012**, *3*, 148-155; d) A. Desmarchelier, M. Raynal, P. Brocorens, N. Vanthuyne, L. Bouteiller, *Chem. Commun.* **2015**, *51*, 7397-7400; e) A. Desmarchelier, B. G. Alvarenga, X. Caumes, L. Dubreucq, C. Troufflard, M. Tessier, N. Vanthuyne, J. Idé, T. Maistriaux, D. Beljonne, P. Brocorens, R. Lazzaroni, M. Raynal, L. Bouteiller, *Soft Matter* **2016**, *12*, 7824-7838.

[24] V. Simic, L. Bouteiller, M. Jalabert, *J. Am. Chem. Soc.* **2003**, *125*, 13148-13154.

[25] A. Timme, R. Kress, R. Q. Albuquerque, H. W. Schmidt, *Chem. Eur. J.* **2012**, *18*, 8329-8339.

[26] F. Lortie, S. Boileau, L. Bouteiller, C. Chassenieux, B. Deme, G. Ducouret, M. Jalabert, F. Laupretre, P. Terech, *Langmuir* **2002**, *18*, 7218-7222.

[27] The radius determined by SANS analysis (r=7.6 Á) is consistent with the half-length of the extended conformation (*ca.* 14 Å) generated by substituting every atoms with spheres having van der Waals radius (Winmostar software). Geometry optimization was performed using through molecular mechanic method (MM3) using the software Scigress (Fujitsu). .

[28] According to SANS analysis the degree of polymerization is more than 275, so that the free N-H fraction due to chain ends should be less than 1%.

[29] Y. P. Zhou, M. Zhang, Y. H. Li, Q. R. Guan, F. Wang, Z. J. Lin, C. K. Lam, X. L. Feng, H. Y. Chao, *Inorg. Chem.* **2012**, *51*, 5099-5109.

[30] a) L. Brunsveld, A. P. H. J. Schenning, M. A. C. Broeren, H. M. Janssen, J. A. J. M. Vekemans, E. W. Meijer, *Chem. Lett.* **2000**, 292-293; b) M. M. J. Smulders, T. Buffeteau, D. Cavagnat, M. Wolffs, A. P. H. J. Schenning, E. W. Meijer, *Chirality* **2008**, *20*, 1016-1022.

[31] P. Jonkheijm, P. van der Schoot, A. P. H. J. Schenning, E. W. Meijer, *Science* **2006**, *313*, 80-83.

[32] M. M. J. Smulders, A. P. H. J. Schenning, E. W. Meijer, *J. Am. Chem. Soc.* **2008**, *130*, 606-611.

[33] C. Kulkarni, E. W. Meijer, A. R. A. Palmans, *Acc. Chem. Res.* **2017**, *50*, 1928-1936.

[34] M. M. Green, J. W. Park, T. Sato, A. Teramoto, S. Lifson, R. L. B. Selinger, J. V. Selinger, *Angew. Chem. Int. Ed.* **1999**, *38*, 3139-3154.

[35] M. M. J. Smulders, P. J. M. Stals, T. Mes, T. F. E. Paffen, A. P. H. J. Schenning, A. R. A. Palmans, E. W. Meijer, *J. Am. Chem. Soc.* **2010**, *132*, 620-626.

[36] a) J. van Gestel, P. van der Schoot, M. A. J. Michels, *Macromolecules* **2003**, *36*, 6668-6673; b) J. van Gestel, *Macromolecules* **2004**, *37*, 3894-3898; c) J. van Gestel, P. van der Schoot, M. A. J. Michels, *J Chem Phys* **2004**, *120*, 8253-8261; d) A. J. Markvoort, H. M. M. ten Eikelder, P. A. J. Hilbers, T. F. A. de Greef, E. W. Meijer, *Nat. Commun.* **2011**, *2*; e) H. M. M. ten Eikelder, A. J. Markvoort, T. F. A. de Greef, P. A. J. Hilbers, *J. Phys. Chem. B* **2012**, *116*, 5291-5301; f) B. Jouvelet, B. Isare, L. Bouteiller, P. van der Schoot, *Langmuir* **2014**, *30*, 4570-4575.

[37] a) P. J. M. Stals, J. C. Everts, R. de Bruijn, I. A. W. Filot, M. M. J. Smulders, R. Martín-Rapún, E. A. Pidko, T. F. A. de Greef, A. R. A. Palmans, E. W. Meijer, *Chem. Eur. J.* **2010**, *16*, 810-821; b) T. Mes, S. Cantekin, D. W. R. Balkenende, M. M. M. Frissen, M. A. J. Gillissen, B. F. M. De Waal, I. K. Voets, E. W. Meijer, A. R. A. Palmans, *Chem. Eur. J.* **2013**, *19*, 8642-8649; c) T. Kim, T. Mori, T. Aida, D. Miyajima, *Chem. Sci.* **2016**, *7*, 6689-6694; d) E. E. Greciano, J. Calbo, J. Buendía, J. Cerdá, J. Aragó, E. Ortí, L. Sánchez, *J. Am. Chem. Soc.* **2019**, DOI: 10.1021/jacs.1029b02045.

[38] Y. F. Zhou, M. Xu, T. Yi, S. Z. Xiao, Z. G. Zhou, F. Y. Li, C. H. Huang, *Langmuir* **2007**, *23*, 202-208.

[39] Intriciate co-assembly behaviour upon mixing different types of discotic monomers has been reported in ref 18b .

[40] B. Adelizzi, A. Aloi, A. J. Markvoort, H. M. M. Ten Eikelder, I. K. Voets, A. R. A. Palmans, E. W. Meijer, *J. Am. Chem. Soc.* **2018**, *140*, 7168-7175.

[41] a) J. Kang, D. Miyajima, T. Mori, Y. Inoue, Y. Itoh, T. Aida, *Science* **2015**, *347*, 646-651; b) B. Narayan, K. K. Bejagam, S. Balasubramanian, S. J. George, *Angew. Chem. Int . Ed.* **2015**, *54*, 13053-13057; c) W. Zhang, W. S. Jin, T. Fukushima, T. Mori, T. Aida, *J. Am. Chem. Soc.* **2015**, *137*, 13792-13795; d) X. J. Ma, Y. B. Zhang, Y. F. Zhang, Y. Liu, Y. K. Che, J. C. Zhao, *Angew. Chem. Int . Ed.* **2016**, *55*, 9539-9543; e) D. S. Pal, H. Kar, S. Ghosh, *Chem. Commun.* **2018**, *54*, 928-931.

[42] C. Edinger, S. R. Waldvogel, *Eur. J. Org. Chem.* **2014**, 5144-5148.

Entry for the Table of Contents (Please choose one layout)

Layout 1:

FULL PAPER

N-substituted benzene-1-urea-3,5-biscarboxamide (BUBA) monomers cooperatively assemble in apolar solvents to give non C_3-symmetric, chirally-amplified, threefold hydrogen-bonded supramolecular helices. The compatibility between the urea and amide functions facilitates the formation of single-handed BUBA – BTA co-assemblies.

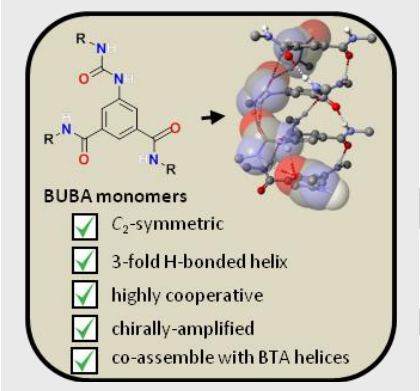

Y. Li, L. Dubreucq, B. G. Alvarenga, M. Raynal, L. Bouteiller*

Page No. – Page No.

_N_-substituted benzene-1-urea-3,5-biscarboxamide (BUBA): easily accessible C_2-symmetric monomers for the construction of reversible and chirally-amplified helical assemblies

Layout 2:

FULL PAPER

*Author(s), Corresponding Author(s)**

Page No. – Page No.

Title

Text for Table of Contents